

Boric Acid Enhances Migration and Cytoskeletal Organization in T98G Cells: Against The Effects of Imatinib

Didem Mimirolu^{1,a,*}, Deniz Çabuk^{2,b}, Merve Akkulak^{2,c}

¹ Department of Biochemistry, Faculty of Science, Sivas Cumhuriyet University, 58140, Sivas, Türkiye

² Department of Biological Sciences, Middle East Technical University, Ankara, Türkiye

*Corresponding author

Research Article

History

Received: 07/04/2025

Accepted: 18/07/2025



This article is licensed under a Creative Commons Attribution-NonCommercial 4.0 International License (CC BY-NC 4.0)

ABSTRACT

Imatinib is one of the Food and Drug Administration approved tyrosine-kinase inhibitors and widely used for the treatment of various cancers. During its use for treatment, mild to moderate side effects which affect neural cells and tissues, are commonly experienced by many patients. Boric acid is a trace element found in living organisms and many beneficial effects on the healing of the damaged cells and tissues are reported in literature. Although there are numerous studies in literature that include individually applications of imatinib and boric acid, there is no study examining their combined effects on T98G glioblastoma cells. Towards this goal, the present study aimed to evaluate the effects of the combined treatment of imatinib (5 μ M) and boric acid (15 mM) on T98G cells. The results showed that cellular migration increased ~2-fold ($p < 0.01$), cellular morphology exhibited a spindle-shaped morphology and MAP2 expression levels and f-actin intensity were ~1.5-fold higher for the combined treatment compared to only imatinib administration. The results cumulatively showed that the adverse effects of imatinib on T98G cells were reduced with boric acid and the biological properties of these cells were improved.

Keywords: Imatinib, Boric acid, Combined treatment, T98G glioblastoma cells.

^a dmimiroglu@cumhuriyet.edu.tr

^c makkulak@metu.edu.tr

^b <https://orcid.org/0000-0003-2838-9719>

^d <https://orcid.org/0000-0003-2834-7682>

^e dcabuk@metu.edu.tr

^f <https://orcid.org/0000-0002-8874-0876>

Introduction

Imatinib mesylate (also known as Glivec in Europe/Latin America/Australia and Gleevec in United States) is one of Food & Drug Administration (FDA) approved tyrosine kinase inhibitor (TKI) which is widely used in the treatment of cancers such as chronic myeloid leukaemia (CML) and gastrointestinal stromal tumor (GIST) [1–3]. Imatinib performs its function by targeting platelet-derived growth factor receptors (PDGFRs), stem-cell factor receptor (c-Kit), and Bcr-Abl fusion transcript [4–6]. However, its clinical beneficial effects in different types of cancers, it has also some adverse effects such as poor blood-brain barrier penetration, optic nerve edema, retinal hemorrhages, demyelinating effect, intracranial bleeding, peripheral neuropathy and pleural and pericardial effusion [5,7–9]. Additionally, among these adverse effects, peripheral neuropathy could be related to disturbance of axonal transport, axonal damage, and mitochondrial dysfunction, the mechanism is not yet fully understood [5]. On the other hand, there are some cases that are reported as demyelination in the central nervous system (CNS) post-initiation of imatinib [10].

Boron is one of the trace elements for organisms and has many significant roles for plants, human health, and animals [11–13]. For humans, the main form of boron is boric acid [12], which has many beneficial effects in the human body, such as enhancing the brain electrical

activities, being neuroprotective, bone growth and maintenance, wound healing, maintenance of sex hormones, anti-inflammatory effects, etc [11,14]. Therefore, boron and its compounds are widely used in pharmaceutical applications [13]. In the literature, many studies related to boric acid, indicate efficient properties for neural cells and tissues as a protective agent. For instance, Ataizi et al. [14] tested the effects of boric acid on traumatic brain injury (TBI) in accordance with evaluating catalase (CAT) activity and levels of malondialdehyde (MDA). It was shown that MDA levels were ~1.5-fold and ~0.5-fold lower for TBI+boric acid compared to TBI without boric acid, respectively [14]. In another study, Ozdemir et al. [15] showed that boric acid had positive effects on the rats with rotenone-induced Parkinson's disease by enhancing motor behaviors, improving neural degeneration, and elevating antioxidant capacity [15].

Although there are many studies in the literature that investigate the effects of imatinib and boric acid on different types of cells and tissues, individually, there are no studies performed with imatinib and boric acid as a combined treatment on T98G glioblastoma cells. Since T98G cell line were used for neuronal marker, neuroinflammation, neurotoxicity studies, creating advanced 3D human brain models, and also evaluating

neuronal cell repair and regeneration processes for neuroscience [16–21], it was preferred in this study. As mentioned before, imatinib may damage tissues due to its side effects such as neurological, dermatological, pancreatic, endocrine and metabolic dysfunctions [7], while boric acid has protective effects on tissues by enhancing cellular mechanisms for different types of cells. Towards this goal, in this research, a combined treatment of imatinib and boric acid was performed to evaluate the effects on T98G cells. Cellular viability via MTT assay, cellular morphology via immunofluorescence imaging, cellular migration via scratch assay, and protein expression levels via western blotting were investigated in treated T98G cells. Evaluating and understanding these findings could be helpful to develop new therapeutic strategies for tyrosine kinase inhibitors, particularly imatinib, while also reducing their side-effects.

Materials And Methods

Sample Preparation for Cytotoxicity Evaluation of Imatinib and Boric Acid

Boric acid (Sigma-Aldrich, Germany) and imatinib (SC-202180, ChemCruz) solutions were prepared with different concentrations in T98G cell growth medium. Boric acid solutions were prepared with 5 mM, 10 mM, 15 mM, 20 mM and 25 mM concentrations. On the other hand, imatinib solutions were prepared with 5 μ M, 10 μ M, 15 μ M, 20 μ M and 25 μ M concentrations. All samples were sterilized with 0.22 μ m membrane filter by using a plastic syringe.

Cell Culture

Human glioblastoma cell line, T98G (ATCC®, CRL-1690™) was used to test biological effects of the boric acid and imatinib *in vitro* due to the widespread use of this cell line in cytotoxicity, adhesion and spreading assays for neuroscience research [16,18,19,21,22]. T98G cells were cultured in Eagle's Minimal Essential Medium (EMEM) (Sigma-Aldrich, Germany) supplemented with 10% fetal bovine serum (FBS) (Sigma-Aldrich, Germany), 1% L-Glutamine (Sigma-Aldrich, Germany) and 1% penicillin-streptomycin (PS) (Sigma-Aldrich, Germany) under 37 °C and 5% CO₂ cell culture conditions as per established protocols [16].

Cell Viability Assay

To assess viability of the cells, Resazurin cell viability assay (39905.01, SERVA, Heidelberg, Germany) was used. Absorption of resazurin causes reduction to resorufin by aerobic respiration of metabolically active cells [23]. T98G cells were cultured on 96-wells culture plate at a density of 2×10^4 cells/cm². After 24 h, seeded cells were treated with different concentrations of imatinib and boric acid for 24 h and 48 h. After the incubation, the growth medium was removed and cells were washed with prewarmed phosphate buffer saline (PBS). The cells were incubated for 4 h in the growth medium supplemented

with 10% resazurin reagent. The absorbances were measured at 570 nm and 600 nm by using Multiskan™ FC Microplate Photometer (Thermo Scientific Multiskan GO). Cell viability experiments were performed three times and eight samples were used in each repeat (biological and technical replicates, respectively).

Immunofluorescence Imaging

The morphology of the T98G cells was evaluated with fluorescence staining using 4',6-diamino-2-phenylindole (DAPI) (Sigma-Aldrich, Germany) and rhodamine-phalloidin staining (ab112127, Abcam) procedures for observing nuclei and actin filaments, respectively [24]. T98G cells were seeded at density of 1×10^4 cell/cm² onto 24-wells culture plate. After that, T98G cells were treated with both imatinib and boric acid solutions with specified concentrations from cell viability assay for 72 h. At the end of 72 h, cells were fixed with 4 % paraformaldehyde for 30 min. The fixed cells were rinsed with 1XPBS and cell membranes were permeated with 0.2 % Triton X-100 for 30 min. 5 % bovine serum albumin (BSA) (Sigma-Aldrich, Germany) prepared in 1XPBS was used both as a blocking solution. Blocking step was applied prior to and after incorporation of the primary antibody solution. For the staining procedure, the permeated cells were initially incubated with rhodamine-phalloidin for 1 h. Once cells were stained for actin filaments, DAPI (0.5 % BSA in 1xPBS, 1:40.000) was used to stain the nuclei 30 min. A fluorescence microscope (EVOS Cell Imaging System, ThermoFisher Scientific, USA) was used to image the cells. Images were quantitatively analyzed using ImageJ software (NIH, Maryland, USA). Immunofluorescence staining experiments were performed three times, and each experiment was repeated with four different samples for each group (biological replicates), and three different images were captured from different parts of each sample (technical replicates).

Protein Expression Levels by Western Blotting

MAP2 protein expression levels were assessed with Western blotting to identify T98G microtubule production. Firstly, T98G cells were seeded onto 24-wells culture plate at a density of 5×10^4 cell/cm². After 24 h, cells were incubated with imatinib and boric acid solutions with specified concentrations for 48 h. After the incubation, cells were lysed using a buffer solution (M-PER™ Mammalian Protein Extraction Reagent, Thermo Fisher Scientific) plus protease inhibitors (Roche Complete Mini EDTA-free, Roche Diagnostic GmbH), followed by centrifuging the lysates at 13.000 rpm for 10 min. The supernatants were assayed for their protein contents with Bradford assay (Pierce™ Coomassie Protein Assay Kit, Thermo Fisher Scientific), while 10 μ g of protein from each extract was analyzed with Western blotting [25]. Afterwards, the nitrocellulose membrane blots were probed with anti-MAP2 (rabbit, 5 % milk in phosphate buffer, 1:1.000, ab32454, Abcam) antibody overnight at 4 °C. Same procedure was repeated for β -actin (rabbit, 5 % milk in phosphate buffer, 1:1.500, PA1183, Thermo Fisher

Scientific) as a loading control. Western blot signal was enhanced by chemiluminescence (Clarity™ Western ECL Substrate, Bio-Rad Laboratories) using goat anti-rabbit IgG coupled to horseradish peroxidase (5 % milk in phosphate buffer, 1:10.000) as the secondary antibody and imaged with a gel imaging system (BIO-RAD ChemiDoc MP Imaging System). The protein band intensities were quantified with ImageJ software (NIH, Maryland, USA). Experiments were repeated for three times with three replicates in each group (both biological and technical replicates).

Scratch Assay

The scratch wound healing assay was performed to evaluate the migration ability of T98G cells after the treatment with imatinib and boric acid solutions [26]. Cells were cultured on 12-wells culture plate until they reached 80–90% confluency. A straight-line scratch was manually introduced vertically in the monolayer with a 1000 μ L pipette tip. The detached cells were removed by gently washing with PBS. After that, imatinib and boric acid solutions prepared in the cell culture medium were added. Cell migration into the wound area was captured at 0 h and 48 h time points using inverted phase-contrast microscope. At the end, the wound closure percentage was analyzed using ImageJ software (NIH, Maryland, USA). All experiments were repeated for three times with five replicates in each group (both biological and technical replicates).

Statistical Analysis

The Shapiro-Wilk test was applied to verify the normality of the results (IBM SPSS Statistics, Version 28), followed by an analysis for statistical significance using ANOVA (IBM SPSS Statistics, Version 28). Tukey's HSD post-hoc test was performed to determine significant differences within groups. Statistical significance was defined as a $p < 0.01$. The values were given as mean \pm standard deviation (SD).

Results And Discussion

To evaluate whether imatinib and boric acid have synergistic effects on the proliferation of T98G cells were treated at different concentrations of imatinib and boric acid alone or together. T98G cell viability profile for boric acid and imatinib alone at 24 h and 48 h was shown in Fig. 1a and 1b. As shown, there was a statistically significant ($**p < 0.01$) decrease in T98G cells for all imatinib groups compared to the control (Fig. 1a) while there was a statistically significant ($**p < 0.01$) decrease in T98G cells for all boric acid groups except 5 mM group compared to the control (Fig. 1b) as early as 24 h post-treatment. The decrease in viable cell numbers became more significant at 48 h for imatinib treatment, especially for higher imatinib concentrations (Fig. 1a). Based on existing knowledge, imatinib is one of the anti-cancer drugs and therefore, these results were in line with literature findings for T98G cells and different cell types, especially at higher imatinib concentrations [27–30]. On the other hand, while a decrease in T98G cellular proliferation was

observed at 24 h post-treatment for the different boric acid concentrations compared to the control group, a subsequent increase in cell number was observed at 48 h post-treatment, especially for 15 mM, 20 mM, and 25 mM boric acid concentrations (Fig. 1b). These results were in line with literature findings at 24 h of boric acid treatments as evaluated in this study [31].

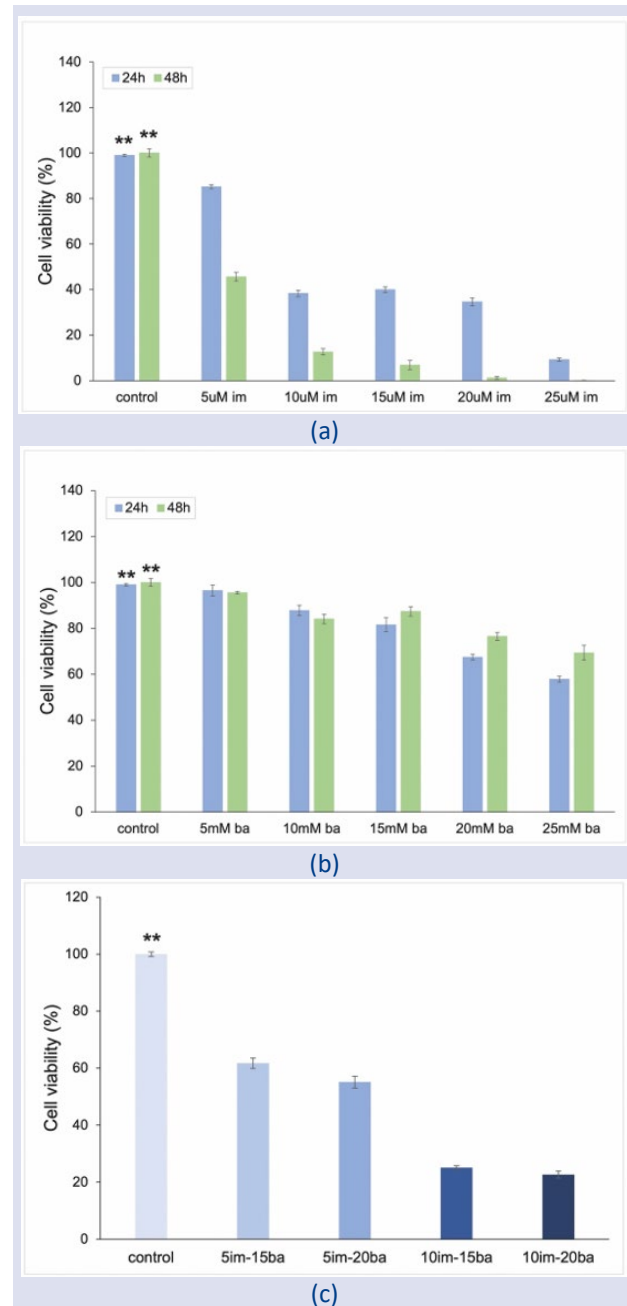


Figure 1. (a) T98G cellular viability profile with imatinib at 24 h and 48 h *in vitro*. (b) T98G cellular viability profile with boric acid at 24 h and 48 h *in vitro*. (c) T98G cellular viability profile with combined treatment at 48 h *in vitro*. Values are mean \pm SD (n=8), $**p < 0.01$.

In combined application, the two doses which were close each other corresponding to half maximal inhibitory concentration 50 (IC₅₀) value were selected for imatinib. On the other hand, the two doses which were close each other corresponding to showed the least cell death

compared to the control group and increased at 48 hours were selected for boric acid. T98G cell viability profile for boric acid and imatinib combined treatment at 48 h were shown in Fig. 1c. It was observed that there was a decrease in the cellular viability of T98G cells for 5im-15ba, 5im-20ba, 10im-15ba and 10im-20ba groups and these were found statistically significant compared to control group ($**p < 0.01$). These findings indicate that there was a significant decrease in T98G cellular viability with combination treatment, while the highest decrease was observed at higher concentrations for both boric acid and imatinib. For the following experiments, the 5im-15ba combination treatment was selected according to showing the highest cellular viability among other concentration combinations. The abbreviations used for each sample group are shown in Table 1.

We explored f-actin filaments which are the major components of the cytoskeleton and stained mostly evaluating cellular internal structure, division, migration and adhesion [32,33]. Thus, the intensity of f-actin filaments was explored by immunofluorescence staining to investigate cellular morphology, adhesion profiles of T98G cells. Immunofluorescence images of T98G cells which were treated with 5-im, 15-ba, and 5im-15ba are shown in Fig. 2.

Table 1. The abbreviations used for the combination treatment of boric acid and imatinib with different concentrations

Samples	Abbreviation for sample groups
5 μ M imatinib	5-im
15 mM boric acid	15-ba
5 μ M imatinib – 15 mM boric acid	5im-15ba
5 μ M imatinib – 20 mM boric acid	5im-20ba
10 μ M imatinib – 15 mM boric acid	10im-15ba
10 μ M imatinib – 20 mM boric acid	10im-20ba

The merged immunofluorescence images show nuclei (blue) and f-actin filaments (red). Imaging results were in line with cellular viability profiles for all studied concentrations via resazurin cell viability assay. T98G cells did not show any distinct morphological changes and had round-shaped morphology without spread (white arrows) for the control and 5-im groups (Fig. 2a). On the other hand, cells had characteristic elongated-spindle shaped cellular morphologies and f-actin filaments of the cells were observed to be distributed peripherally for 15-ba and 5im-15ba groups (white arrows, Fig. 2a).

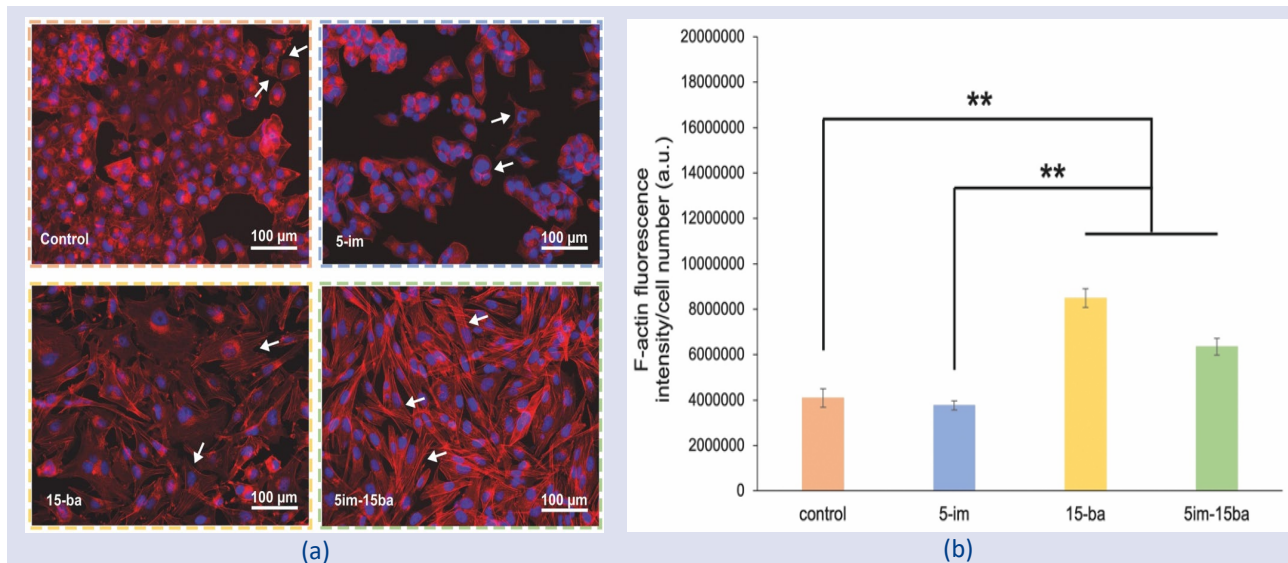


Figure 2. T98G cells stained with DAPI for nuclei (blue), and phalloidin for f-actin filaments (red). (a) The merged immunofluorescence images of the cells with each treatment groups after 72 h of incubation. Scale bars are 100 μ m. (b) The f-actin fluorescence intensity per cell for the cells treated with each groups. Values are mean \pm SD (n=4), $**p < 0.01$.

Additionally, f-actin fluorescence intensities of T98G cells for each treatment groups were analyzed with ImageJ and the results were given in Fig. 2b. It was found that f-actin intensities of the cells with 15-ba and 5im-15ba treatment groups were significantly higher than both control and 5-im groups ($**p < 0.01$). Expression levels of microtubule-associated protein 2 (MAP2) were determined by Western blotting in Fig. 3. The intensity of MAP2 protein expression was normalized and found to be 1.10 ± 0.08 , 0.78 ± 0.26 , 0.93 ± 0.02 and 1.12 ± 0.06 (a.u.) for control, 5-im, 15-ba and 5im-15ba groups, respectively. It

was observed that T98G cells treated with the combination of 5im-15ba showed higher MAP2 protein expression level compared to 5-im and 15-ba alone. MAP2 protein is a dendritically enriched protein and widely used for a specific marker for neural differentiation, neural outgrowth and additionally, for evaluating neural plasticity which is the reorganization of the nervous system due to different types of stimuli [34–36]. Therefore, MAP2 expression levels, shown in Fig. 3b, indicated that boric acid enhanced microtubule formation and stability of T98G cells compared to other groups.

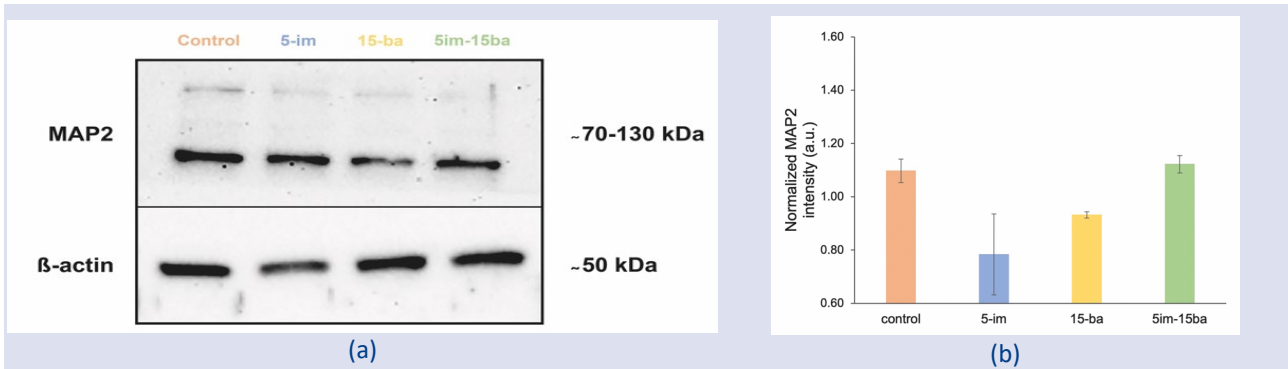


Figure 3. (a) Immunoblot images of control, 5-im, 15-ba, and 5im-15ba treated groups using anti-MAP2 and anti-β-actin. (b) Normalized MAP2 intensity levels for control and all treatment groups. The values are mean±SD, n=3.

The scratch wound healing assay *in vitro* was studied to evaluate the effects of combined treatment based on the migration properties of T98G cells (Fig. 4) [37,38]. As shown in Fig. 4a, similar to proliferation rates, the highest coverage area was demonstrated with 15-ba treatment at 48 h which promoted significant cellular migration compared to control and other groups (** $p < 0.01$). On the contrary, the least coverage area was observed for 5-im group at 48 h which significantly inhibited cellular migration compared to all other groups (** $p < 0.01$). Additionally, wound closure was enhanced about ~2-fold

with the combined treatment, 5im-15ba due to migration compared to 5-im group, and it was found statistically significant (** $p < 0.01$). These results were in line with literature findings which were also found for human keratinocyte cell line (HaCaT) and human primary epithelial cell line (HS-2) [39,40]. As many research indicated that boric acid could have protective effects against DNA damage in the cells, reducing oxidative stress and promoting wound healing via cellular migration [40] which were confirmed by these results.

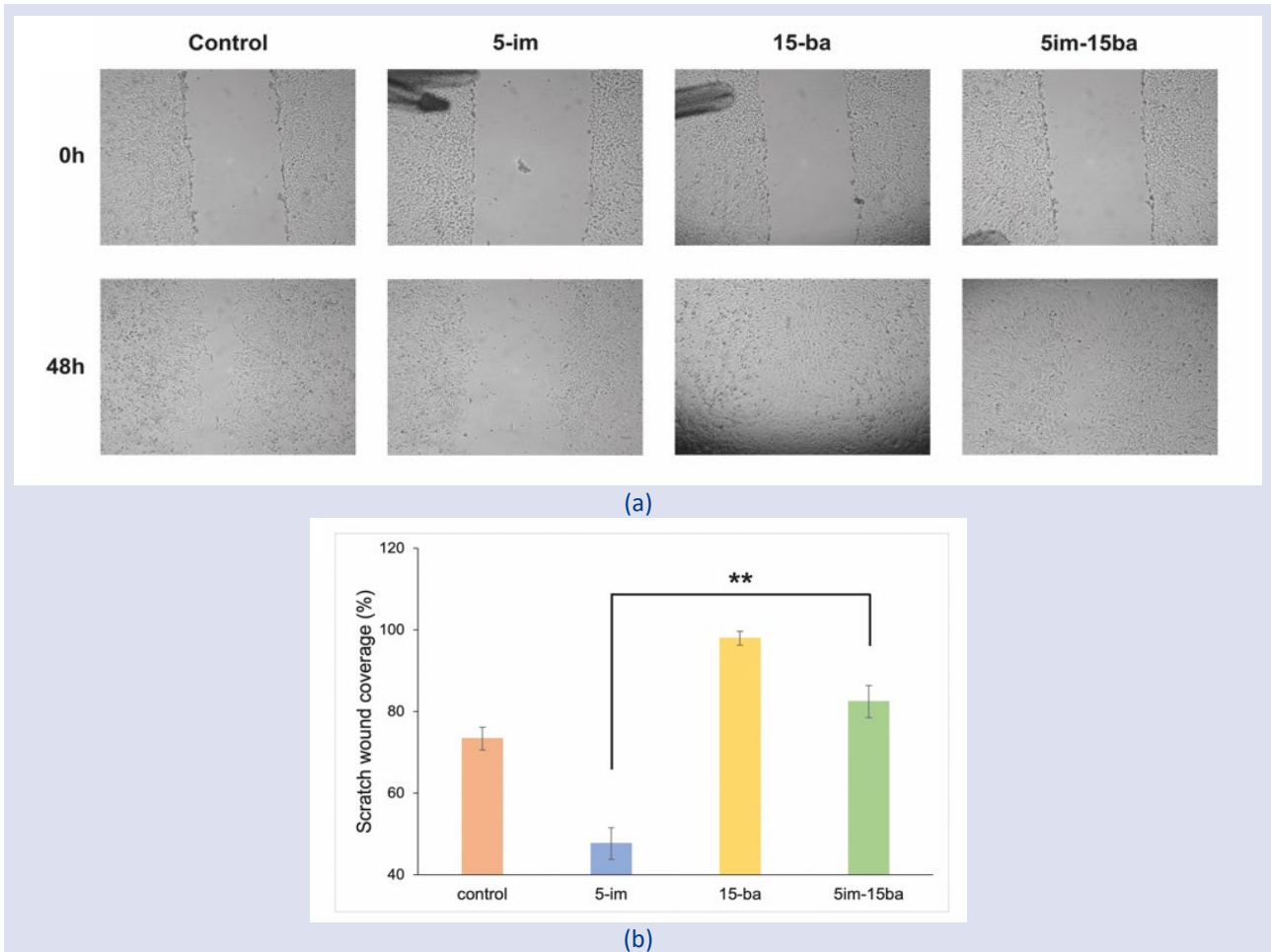


Figure 4. (a) Immunoblot images of control, 5-im, 15-ba, and 5im-15ba treated groups using anti-MAP2 and anti-β-actin. (b) Normalized MAP2 intensity levels for control and all treatment groups. The values are mean±SD, n=3.

To sum up, our results confirmed that the side effects of imatinib treatment on T98G cells could be reduced when it is combined treated with boric acid that facilitating a beneficial effect on the cellular viability, morphology, spreading and migration of the cells. T98G cellular viability, migration, f-actin expression and MAP2 expression increased upon combined treatment of imatinib and boric acid. These observations are predicted to contribute for the developing of new treatment methodologies in which areas of applied imatinib treatment.

Conclusion

The study demonstrates that the combination of imatinib and boric acid reduces the adverse effects of imatinib while enhancing migration and expression of cytoskeletal markers in T98G cells. Although the findings provide promising evidence for cellular protective effects, *in vitro* design via cell line, limited dose range and absence of molecular pathway analysis represent key limitations for the study. Therefore, multiple cell types, *in vivo* models, molecular pathway-specific analysis should be essential and studied as a future project to validate the therapeutic potential of this combination. So, they could have the potential developing for future applications.

Conflicts of Interest

There are no conflicts of interest in this work.

Acknowledgments

The authors would like to thank Biological Sciences Department of METU and Orhan Adalı's Laboratory in METU-Biological Sciences Department for the all experiments.

References

- [1] Ertmer A., Huber V., Gilch S., Yoshimori T., Erfle V., Duyster J., Elsässer H.P., Schälz H.M., The Anticancer Drug Imatinib Induces Cellular Autophagy, *Leukemia*, 21 (5) (2007) 936–942.
- [2] Kim K.J., Jung J.M., Cho J.Y., Woo S.Y., Cho K.A., Ryu K.H., Yoo E.S., Antitumor Effects of Imatinib Mesylate and Synergistic Cytotoxicity with an Arsenic Compound in Neuroblastoma Cell Lines, *Exp. Ther. Med.*, 2 (3) (2011) 557–561.
- [3] Al-Hadiya B.M.H., Bakheit A.H.H., Abd-Elgalil A.A., *Imatinib Mesylate*. In: Profiles of Drug Substances, Excipients and Related Methodology, 1st ed. Elsevier Inc., (2014) 265–297.
- [4] Kumar M., Kulshrestha R., Singh N., Jaggi A.S., Expanding Spectrum of Anticancer Drug, Imatinib, in the Disorders Affecting Brain and Spinal Cord, *Pharmacol. Res.*, 143 (2019) 86–96.
- [5] Jain P., Konoplev S., Benjamini O., Romagura J., Burger J.A., Long-Term Control of Refractory Follicular Lymphoma After Treatment of Secondary Acute Promyelocytic Leukemia with Arsenic Trioxide (As₂O₃) and All-Trans Retinoic Acid (ATRA), *Blood Res.*, 53 (2) (2018) 169–172.
- [6] Aras Y., Erguven M., Aktas E., Yazihan N., Bilir A., Antagonist Activity of the Antipsychotic Drug Lithium Chloride and the Antileukemic Drug Imatinib Mesylate During Glioblastoma Treatment In Vitro, *Neurol. Res.*, 38 (9) (2016) 766–774.
- [7] Shyam Sunder S., Sharma U.C., Pokharel S., Adverse Effects of Tyrosine Kinase Inhibitors in Cancer Therapy: Pathophysiology, Mechanisms and Clinical Management, *Signal Transduct. Target. Ther.*, 8 (1) (2023) 262.
- [8] Schiff D., Wen P.Y., van den Bent M.J., Neurological Adverse Effects Caused by Cytotoxic and Targeted Therapies, *Nat. Rev. Clin. Oncol.*, 6 (10) (2009) 596–603.
- [9] Lixi F., Giannaccare G., Salerno G., Gagliardi V., Pellegrino A., Vitiello L., Side Effects of Novel Anticancer Drugs on the Posterior Segment of the Eye: A Review of the Literature, *J. Pers. Med.*, 14 (12) (2024) 1160.
- [10] Rotstein D.L., Sawicka K., Bharatha A., Montalban X., Lipton J.H., CNS Demyelination After Initiating the Tyrosine Kinase Inhibitor Imatinib: A Report of Two Cases, *Mult. Scler. J.*, 26 (9) (2020) 1121–1124.
- [11] Pizzorno L., Nothing Boring About Boron, *Integr. Med.: A Clinician's Journal*, 14 (4) (2015) 35–48.
- [12] Hilal B., Eldem A., Oz T., Pehlivan M., Pirim I., Boric Acid Affects Cell Proliferation, Apoptosis, and Oxidative Stress in ALL Cells, *Biol. Trace Elem. Res.*, 202 (8) (2024) 3614–3622.
- [13] Turkez H., Alper F., Bayram C., Baba C., Yıldız E., Saracoglu M., Kucuk M., Gozegir B., Kiliclioglu M., Yesilyurt M., Tozlu O.O., Bolat I., Yildirim S., Barutcgil M.F., Isik F., Kiki Ö., Aydın F., Arslan M.E., Cadirci K., Karaman A., Tatar A., Hacimuftuoglu A., Boric Acid Impedes Glioblastoma Growth in a Rat Model: Insights from Multi-Approach Analysis, *Med. Oncol.*, 42 (2) (2025) 1–17.
- [14] Ataizi Z.S., Ozkoc M., Kanbak G., Karimkhani H., Donmez D.B., Ustunisik N., Ozturk B., Evaluation of the Neuroprotective Role of Boric Acid in Preventing Traumatic Brain Injury-Mediated Oxidative Stress, *Turk. Neurosurg.*, 31 (4) (2021) 493–499.
- [15] Ozdemir H.S., Yunusoglu O., Sagmanligil V., Yasar S., Colcimen N., Goceroglu R.T., Catalkaya E., Investigation of the Pharmacological, Behavioral and Biochemical Effects of Boron on Rats with Rotenone-Induced Parkinson's Disease, *Cell. Mol. Biol.*, 68 (8) (2022) 13–21.
- [16] Kiseleva, L. N., Kartashev, A. V., Vartanyan, N. L., Pinevich, A. A., Samoilovich, M. P. A172 and T98G cell lines characteristics. *Cell and Tissue Biology*, 10 (5) (2016) 341–348.
- [17] Kiseleva, L. N., Kartashev, A. V., Vartanyan, N. L., Pinevich, A. A., Filatov, M. V., Samoilovich, M. P. Characterization of new human glioblastoma cell lines. *Cell and Tissue Biology*, 12 (1) (2018) 1–6.
- [18] Fuster, E., Candela, H., Estévez, J., Vilanova, E., Sogorb, M. A. A Transcriptomic Analysis of T98G Human Glioblastoma Cells after Exposure to Cadmium-Selenium Quantum Dots Mainly Reveals Alterations in Neuroinflammation Processes and Hypothalamus Regulation. *International Journal of Molecular Sciences*, 23 (4) (2022) 2267.
- [19] Fabbri, R., Cacopardo, L., Ahluwalia, A., Magliaro, C. Advanced 3D models of human brain tissue using neural cell lines: state-of-the-art and future prospects. *Cells*, 12 (8) (2023) 1181.
- [20] de Joannon, A. C., Mancini, F., Landolfi, C., Soldo, L., Leta, A., Ruggieri, A., Mangano, G., Polenzani, L., Pinza, M., Milanese, C. Adenosine triphosphate affects interleukin-

- 1 β release by T98G glioblastoma cells through a purinoceptor-independent mechanism. *Neuroscience Letters*, 285 (3) (2000) 218-222.
- [21] Fuster, E., Candela, H., Estévez, J., Arias, A. J., Vilanova, E., Sogorb, M. A. Effects of silver nanoparticles on T98G human glioblastoma cells. *Toxicology and Applied Pharmacology*, 404, (2020) 115178.
- [22] Perego C., Vanoni C., Massari S., Raimondi A., Pola S., Cattaneo M.G., Francolini M., Vicentini L.M., Pietrini G., Invasive Behaviour of Glioblastoma Cell Lines is Associated with Altered Organisation of the Cadherin-Catenin Adhesion System, *J. Cell Sci.*, 115 (16) (2002) 3331–3340.
- [23] Al-Nasiry, S., Geusens, N., Hanssens, M., Luyten, C., & Pijnenborg, R. The use of Alamar Blue assay for quantitative analysis of viability, migration and invasion of choriocarcinoma cells. *Human reproduction*, 22 (5) (2007) 1304-1309.
- [24] Mimioglu, D., Tufan, Y., Yanik, T., & Ercan, B. Synergistic effect of nanostructured topography and CNF incorporation into silk fibroin films enhances mouse neuroblastoma cell functions. *Surfaces and Interfaces*, 45 (2024) 103876.
- [25] Mahmood, T., Yang, P. C. Western blot: technique, theory, and trouble shooting. *North American journal of medical sciences*, 4 (9) (2012) 429.
- [26] Vang Mouritzen M., Jenssen H., Optimized Scratch Assay for In Vitro Testing of Cell Migration with an Automated Optical Camera, *J. Vis. Exp.*, 138 (2018) 57691.
- [27] Lu J., Hu Y., Qian R., Zhang Y., Yang X., Luo P., Enhanced Proliferation Inhibition and Apoptosis in Glioma Cells Elicited by Combination of Irinotecan and Imatinib, *Eur. J. Pharmacol.*, 874 (2020) 173022.
- [28] Ren H., Tan X., Dong Y., Giese A., Chou T.C., Rainov N., Yang B., Differential Effect of Imatinib and Synergism of Combination Treatment with Chemotherapeutic Agents in Malignant Glioma Cells, *Basic Clin. Pharmacol. Toxicol.*, 104 (3) (2009) 241–252.
- [29] Ranza E., Mazzini G., Facoetti A., Nano R., In-Vitro Effects of the Tyrosine Kinase Inhibitor Imatinib on Glioblastoma Cell Proliferation, *J. Neurooncol.*, 96 (2010) 349–357.
- [30] Demestre M., Herzberg J., Holtkamp N., Hagel C., Reuss D., Friedrich R.E., Kluwe L., Von Deimling A., Mautner V.F., Kurtz A., Imatinib Mesylate (Glivec) Inhibits Schwann Cell Viability and Reduces the Size of Human Plexiform Neurofibroma in a Xenograft Model, *J. Neurooncol.*, 98 (2010) 11–19.
- [31] Turkez H., Arslan M.E., Tatar A., Mardinoglu A., Promising Potential of Boron Compounds Against Glioblastoma: In Vitro Antioxidant, Anti-Inflammatory and Anticancer Studies, *Neurochem. Int.*, 149 (2021) 105137.
- [32] Melak M., Plessner M., Grosse R., Actin Visualization at a Glance, *J. Cell Sci.*, 130 (3) (2017), 525–530.
- [33] Zonderland J., Wieringa P., Moroni L., A Quantitative Method to Analyse F-Actin Distribution in Cells, *MethodsX*, 6 (2019) 2562–2569.
- [34] Glushakova O.Y., Glushakov A.V., Mannix R., Miller E.R., Valadka A.B., Hayes R.L. The Use of Blood-Based Biomarkers to Improve the Design of Clinical Trials of Traumatic Brain Injury. In: *Handbook of Neuroemergency Clinical Trials*. 2nd ed. Elsevier, (2017) 139-166.
- [35] Mondello S., Hayes R.L., Biomarkers. In: *Handbook of Clinical Neurology*, Vol. 127. Elsevier, (2015) 245–265.
- [36] Mondello S., Gabrielli A., Catani S., D'Ippolito M., Jeromin A., Ciaramella A., Bossù P., Schmid K., Tortella F., Wang K.K.W., Hayes R.L., Formisano R., Increased Levels of Serum MAP-2 at 6-Months Correlate with Improved Outcome in Survivors of Severe Traumatic Brain Injury, *Brain Inj.*, 26 (13-14) (2012) 1629–1635.
- [37] Grada A., Otero-Vinas M., Prieto-Castrillo F., Obagi Z., Falanga V., Research Techniques Made Simple: Analysis of Collective Cell Migration Using the Wound Healing Assay, *J. Invest. Dermatol.*, 137 (2) (2017) e11–e16.
- [38] Stamm A., Reimers K., Strauß S., Vogt P., Scheper T., Pepelanova I., In Vitro Wound Healing Assays – State of the Art, *BioNanoMaterials*, 17 (1-2) (2016) 79–87.
- [39] Demirci S., Doğan A., Aydın S., Dülger E.Ç., Şahin F., Boron Promotes Streptozotocin-Induced Diabetic Wound Healing: Roles in Cell Proliferation and Migration, Growth Factor Expression, and Inflammation, *Mol. Cell. Biochem.*, 417 (2016) 119–133.
- [40] Tepedelen B.E., Soya E., Korkmaz M., Boric Acid Reduces the Formation of DNA Double Strand Breaks and Accelerates Wound Healing Process, *Biol. Trace Elem. Res.*, 174 (2016) 309–318.